THE ELECTRON BUBBLE IN LIQUID HELIUM

P. H. Roberts
University of Newcastle upon Tyne,
Newcastle upon Tyne, NE1 7RU, England

ABSTRACT

The bose condensate model of helium is used to examine the structure of the electron bubble in helium. The solution obtained makes use of the fact that the parameter $(am/\ell M)^{1/5}$ is small and m/M is negligible, where m is the electron mass, M is the boson mass, ℓ is the electron-boson scattering length, and a is the healing length. It is shown that, to leading order, the radius of the bubble is $b = (\pi M^2 a^2/m\rho_\infty)^{1/5}$, when ρ_∞ is the helium density. The effects of (quantum) surface tension and of polarization are discussed, and are shown to be small. Consideration is given to the effective mass and radius of the bubble, and the ellipticity induced in it by slow motion is given. The normal modes of pulsation of the bubble are found and the mobility of the ion is computed. The theory is compared with experiment.

1. INTRODUCTION

It has become increasingly apparent over the past decade that the deliberately introduced impurity can be a fruitful experimental probe of the structure and dynamics of helium II, the superfluid phase of helium. Of particular interest is the negative ion which consists of an electron that, through its zero point motion, carves out a soft bubble of about 16Å in radius in the surrounding helium (1Å = 10^{-8}cm.). The induced hydrodynamic mass of such a large structure is greatly in excess of its physical mass, and it therefore responds to applied forces as would a much more massive ion. The experimental situation has been reviewed by Donnelly[1], and more recently by Fetter[2].

The negative ion provides an interesting and, as we shall see, a sensitive testing ground for theories of helium II. We examine in this paper one particularly simple model of helium near absolute zero, the bose condensate. The approach is expounded by, for example, Gross[3] and by Fetter and Walecka[4]. The theory is so simple to apply that most of the properties of the electron bubble can be calculated in an elementary way. We will present our arguments in a hydrodynamic framework originally proposed by Madelung[5]. Since this may be unfamiliar to the reader, it is developed in §2 for the simple single-particle Schrödinger equation. It is generalized in §3 to the bose condensate. The two theories are brought together in §4, where the theory of the electron bubble is developed. The final section (§5) confronts the theory with experiment.

2. MADELUNG'S TRANSFORMATION

It appears to have been Madelung[5] who first realized that Schrödinger's equation could be cast into a fluid mechanical mold, by expressing the wavefunction, $\psi(\vec{x},t)$, in terms of its amplitude, $f(\vec{x},t)$, and phase, $\phi(\vec{x},t)$. Consider a particle of mass m in a field of fixed potential, $w(\vec{x})$, and therefore obeying

$$i\hbar\partial\psi/\partial t = -(\hbar^2/2m)\ \nabla^2\psi + w\psi. \tag{1}$$

By writing

$$\psi = f\ \exp\ (im\phi/\hbar), \tag{2}$$

where f and ϕ are real, we can divide (1) into

$$2\frac{\partial f}{\partial t} + f\nabla^2\phi + 2\vec{\nabla}f\cdot\vec{\nabla}\phi = 0, \tag{3}$$

$$\frac{\partial\phi}{\partial t} + \frac{1}{2}(\vec{\nabla}\phi)^2 + \frac{w}{m} - \frac{\hbar^2}{2m^2}\frac{\nabla^2 f}{f} = 0. \tag{4}$$

When we introduce the (probabilistic) mass density, ρ, and current $\vec{j}$, by writing

$$\rho = m|\psi|^2 = mf^2, \quad \vec{j} = (\hbar/2i)(\psi^*\vec{\nabla}\psi - \psi\vec{\nabla}\psi^*) = \rho\vec{\nabla}\phi, \tag{5}$$

and define a velocity, $\vec{u}$, by their ratio

$$\vec{u} = \vec{j}/\rho = \vec{\nabla}\phi, \tag{6}$$

we recognize that (3) and (4) are the continuity and momentum equations governing the potential flow (6):

$$\frac{\partial\rho}{\partial t} + \vec{\nabla}\cdot(\rho\vec{u}) = 0, \tag{7}$$

$$\frac{\partial\phi}{\partial t} + \frac{1}{2}\vec{u}^2 + \frac{w}{m} + \mu = 0, \tag{8}$$

where

$$\mu = -(\hbar^2/2m^2)\nabla^2\rho^{1/2}/\rho^{1/2}. \tag{9}$$

There are three main differences from classical potential flow. First, the total quantity of 'fluid' is not only conserved by (7): it is fixed by

$$\int|\psi|^2 d\vec{x} = 1, \quad \text{or} \quad \int\rho d\vec{x} = m. \tag{10}$$

Second, even if through the presence of walls ($w=\infty$) or otherwise the fluid is confined to a certain multiply-connected domain, $\mathcal{R}$, ψ must remain single-valued. It follows from (2) that, round any contour Γ in $\mathcal{R}$ not reducible to a point by a continuous deformation, ϕ can change by a multiple of h/m only. The circulation round Γ cannot freely take any value: it is quantized by the Bohr-Sommerfeld condition

$$\oint_\Gamma \vec{u}\cdot d\vec{x} = \frac{nh}{m}, \quad (n=0, \pm1, \pm2.....). \tag{11}$$

Third, a completely new term has appeared in the momentum equation (8), namely μ.

The term μ is often called 'the quantum pressure'. This is a misnomer for at least three reasons. First, its dimensionality is incorrect, and it would be better regarded as a chemical potential per unit mass. Second, since

$$\partial\mu/\partial x_i = -\rho^{-1}\partial\sigma_{ij}/\partial x_j, \tag{12}$$

where[6-8]

$$\sigma_{ij} = \frac{\hbar^2}{2m^2}\rho\frac{\partial^2}{\partial x_i\partial x_j}(\ln\rho^{1/2}), \tag{13}$$

a rival, and properly dimensioned, contender for the title of quantum pressure exists as part of the unusual and complicated stress tensor (13). Third, the word 'pressure' suggests a phenomenon that depends only on 'the local thermodynamic state' (here fixed by ρ), and the presence of derivatives in (9), or (13), shows that all neighboring points are involved in its definition. Despite these objections, we follow the common usage.

As may be seen by setting $\hbar = 0$ in (9), the quantum pressure is the essential ingredient that distinguishes our subject from the classical theory. The fluid dynamicist can gather experience of its effects by translating some of the elementary situations of quantum theory into their corresponding fluid mechanical statements.

'Hydrostatics' arises from the quantum mechanical bound states by writing

$$\phi = -Et, \tag{14}$$

where E, the energy of the state, is a constant. By (8) the quantum pressure balances E-w everywhere. It is best to avoid the usual fluid mechanical practice of absorbing E into w, since some energy levels may be inaccessible. For example, when (8) is written as

$$-(\hbar^2/2m)\ \nabla^2 f = [E - w(\vec{x})]f, \tag{15}$$

and it is supposed that w increases indefinitely with distance, r, from some origin, 0, one family of solutions to (15) is found that increase with r, so that the normalization integrals (10) do not converge. The condition that only the normalizable solutions of the other family are used transforms (15) into an eigenvalue problem that confines E to discrete levels. Of course a continuum of eigenvalues exists when w is bounded above.

A well-known application of (15), that is particularly relevant to the bubble, is the potential well for which

$$w = \begin{cases} w_I, \text{ in } r<b \text{ ('Region I')}; \\ w_{II}, \text{ in } r>b \text{ ('Region II')}; \end{cases} \tag{16}$$

where w_I and w_{II} ($>w_I$) are constants. Writing

$$\lambda_I^2 = (2m/\hbar^2)\ (E - w_I), \qquad \lambda_{II}^2 = (2m/\hbar^2)(w_{II} - E), \tag{17}$$

we see that, for $w_I < E < w_{II}$, (15) is obeyed by

$$f = f_I \equiv Aj_\ell(\lambda_I r)\ Y_\ell(\theta,\chi), \text{ in } r \le b; \tag{18}$$

$$f = f_{II} \equiv Ak_\ell(\lambda_{II} r)[j_\ell(\lambda_I b)/k_\ell(\lambda_{II} b)]\ Y_\ell(\theta,\chi), \quad \text{in } r \ge b; \tag{19}$$

where $j_\ell(z)$ is the spherical Bessel function of the first kind, $k_\ell(z)$ is the modified spherical Bessel function of the second kind, and $Y_\ell(\theta,\chi)$ is a surface harmonic of integral degree, ℓ, in spherical coordinates (r, θ, χ). The exclusion of the other spherical Bessel functions ensures that (10) can be met for some choice of the constant A. Continuity of f has been realized, and $\vec{\nabla}f$ is continous provided

$$\lambda_I b j_\ell'(\lambda_I b)/j_\ell(\lambda_I b) = \lambda_{II} b k_\ell'(\lambda_{II} b)/k_\ell(\lambda_{II} b). \tag{20}$$

This dispersion relationship determines a discrete spectrum of admissible E. It may be seen that, when $\Delta w \equiv w_{II} - w_I$ is large compared with h^2/mb^2, eigensolutions exist for which $E - w_I \ll w_{II} - E$. For these, (19) takes the approximate form

$$f_{II} \doteq A \exp[-\lambda_{II}(r - b)]\ Y_\ell(\theta,\chi), \quad \text{in } r \ge b. \tag{21}$$

The fluid is confined in region II to a boundary layer of thickness $1/\lambda_{II}$, or

$$a_m = \hbar\ (2m\Delta w)^{-1/2}. \tag{22}$$

This phenomenon is often called 'healing', the layer itself a 'healing layer', and a_m the 'healing length'. To the fluid mechanicist, the abrupt increase Δw in w at r = b can only be hydrostatically balanced by an equally abrupt increase in quantum pressure. It is the non-local character of quantum pressure that causes the fluid to pass through the barrier at r = b and, when lower potentials are available externally, permits it to seep out of region I.

In view of later developments, it is worth elaborating the situation just described. First we allow the well to have any shape, defining n to be a coordinate that measures distance from the discontinuity normally outwards from I to II. Second, we allow w_I and w_{II} to vary, and suppose that the large transition from w_I up to w_{II} does not occur abruptly as in (16), but continuously over some distance, a, comparable with a_m. Within this distance, there is evidently no unique way of defining 'the' surface, S, of the well. We note, however, that in the case of discontinuous w just considered, $j_\ell(\lambda_I b)$ is small, by (20). This suggests we should locate S on the surface of zero f_I.

To elucidate the healing layer structure, we introduce a stretched coordinate, ξ, and cast (15) into dimensionless form by writing

$$\xi = n/a, \qquad f = ax(\xi), \tag{23}$$
$$q = a/a_m, \qquad w = w_I + g(\xi)\Delta w, \tag{24}$$

where we suppose g is exponentially small at the inner ($\xi = -\infty$) edge of the boundary layer, and is unity at the outer ($\xi = +\infty$) edge. It should be realized that x, w_I, Δw and g will generally depend on position on S. To the first two orders, however, this dependence only occurs parametrically in the solution, and will therefore be suppressed. Writing

$$x = x_o(\xi) + ax_1(\xi) + \ldots, \tag{25}$$

substituting into (15), and equating like powers of a, we obtain

$$d^2x_o/d\xi^2 - q^2 g(\xi)x_o = 0, \tag{26}$$

$$d^2x_1/d\xi^2 - q^2 g(\xi)x_1 = -(C_1^{-1} + C_2^{-1})dx_o/d\xi, \tag{27}$$

where C_1 and C_2 are the principal radii of curvature of S at the point concerned. Since f_{II} is identically zero, the solutions to (26) and (27) must obey

$$x_o \to 0, \quad x_1 \to 0, \quad \text{for } \xi \to +\infty. \tag{28}$$

Successful matching to the interior solution, f_I, requires

$$x_o \sim (\partial f_I/\partial n)_S\xi, \quad x_1 \sim -\tfrac{1}{2}(C_1^{-1} + C_2^{-1})(\partial f_I/\partial n)_S\xi^2, \quad \text{for } \xi \to -\infty. \tag{29}$$

Explicit solutions can generally be obtained only by numerical means. They obey integral conditions which we will later find useful (§4):

$$\frac{1}{q^2}\left(\frac{\partial f_I}{\partial n}\right)_S^2 = \int_{-\infty}^{\infty} x_o^2 \frac{dg}{d\xi}\, d\xi, \tag{30}$$

$$-\frac{2}{q^2}\left(\frac{1}{C_1} + \frac{1}{C_2}\right) ⨍_{-\infty}^{\infty}\left(\frac{dx_o}{d\xi}\right)^2 d\xi = \int_{-\infty}^{\infty} 2x_o x_1 \frac{dg}{d\xi}\, d\xi, \tag{31}$$

where the bar through the integral sign signifies that the convergent part of the integral is taken. Despite appearances, this integral is negative.

The integral relationships (30) and (31) may be interpreted in the light of the Grant tensor (13). The terms on the left give the main parts of the leap of σ_{nn} across the boundary layer; the terms on the right give the corresponding integrated effects of the external force $f^2\nabla w$ balancing them. The dominant term, given on the left of (30), arises from the 'pressure' of the particle trying to escape the well. The next largest term, shown on the left of (31), clearly has the form of a quantum surface stress, with

$$T_m = \frac{2a\Delta w}{q^2} \int_{-\infty}^{\infty}(a\,\frac{dx_0}{d\xi})^2 d\xi \quad . \tag{32}$$

as coefficent of surface tension. It is easy to make an estimate of T_m. If we take g to be a unit step function, we find from (26) that

$$T_m \doteq -a_m{}^3\Delta w\ (\partial f_I/\partial n)^2_S. \tag{33}$$

Passing from 'hydrostatics' to 'hydrodynamics' by abandoning (14), we see from (8) that another type of healing phenonmenon will occur when u is large. A particularly significant case occurs at a vortex line where, by (11), u is of order $nh/m\tilde{\omega}$, at small distances, $\tilde{\omega}$, from the vortex axis. It follows from (8) and (9) that ρ is of order $\tilde{\omega}^{2n}$ for $\tilde{\omega} \to 0$. The fact that ρ is zero on the axis itself means that a closed vortex ring, or a vortex line terminating on boundaries ($w = \infty$), will transform an otherwise simply-connected container into a multiply-connected domain, $\mathcal{R}$, so justifying a posteriori the application of (11). Unlike the healing at a wall considered earlier, the depression of ρ at the vortex axis occurs over distances comparable with the scale of the container. The corresponding vortices in the condensate discussed in §3 have cores confined to much smaller distances from their axes.

Before concluding this section we make one remark, obvious perhaps, but relevant to §4. When the particle is trapped in a potential well with moving walls [$w = w(\vec{x},t)$], ϕ is necessarily non-zero and ρ is time-dependent. Nevertheless, provided the time-scales over which w changes are large compared with the reciprocal of the quantum frequency h/mb^2, we can regard the fluid as being in a quasi-hydrostatic state, ignore the time derivative in (1), and treat t in w parametrically. In quantum language, the Born-Oppenheimer approximation is said to apply.

3. THE CONDENSATE MODEL

We now consider an assembly of N identical particles (bosons) of mass M in a potential field $W(\vec{x})$. If the particles did not interact, the wavefunction for the system could be written down as a symmetrized product of the N one-particle wavefunctions, $\Psi(\vec{x},t)$, obeying (11) with W and M replacing w and m. It would be probably more convenient, however, to replace the normalization condition (10) by

$$\int|\Psi|^2 d\vec{x} = N, \quad \text{or} \quad \int\rho d\vec{x} = \rho_\infty v, \tag{34}$$

where v is the volume of the system and $\rho_\infty = MN/v$. The resulting theory is well-understood, and contains features that fruitfully represent helium near absolute zero[8]. It may be seen from (18), however, that the ground state for, say, the potential well (16) would be one in which all the particles would be at the origin, with high probability. To eliminate this unphysical behavior, the imperfect bose condensate has been devised. A short-range repulsive potential $V(\vec{x} - \vec{x}')$ is introduced in an ad hoc way, and to W the potential

$$\int V(\vec{x} - \vec{x}')\,|\Psi(\vec{x}')|^2 d\vec{x}' \tag{35}$$

is added which increases as the density of nearby bosons increases. The simplest case arises when V is taken to be

$$V(\vec{x} - \vec{x}') = V_o\,\delta(\vec{x} - \vec{x}'). \tag{36}$$

Equation (1) is then replaced by

$$i\hbar\partial\Psi/\partial t = -(\hbar^2/2M)\nabla^2\Psi + (V_o|\Psi|^2 + W)\Psi. \tag{37}$$

A fuller and more satisfactory derivation of (37) may be found elsewhere[3,4]. It is of some interest that non-linear Schrödinger equations of the form (37) have been the subject of close scrutiny in recent years in non-quantal contexts, particularly in theories of weak non-linear waves and stability[9]. The Madelung transformation

$$\Psi = F\exp(iM\Phi/\hbar), \tag{38}$$

follows the course of §2 with minor changes. Most significant is the addition of a 'gas pressure',

$$p = (V_o/2M^2)\rho^2, \tag{39}$$

which (multiplied by δ_{ij}) should be included in the stress tensor (13). Thus (8) is replaced by

$$\frac{\partial\Phi}{\partial t} + \frac{1}{2}\vec{u}^2 + \frac{W}{M} + \frac{2p}{\rho} + \mu = 0. \tag{40}$$

The presence of the repulsion, V_o, and its associated gas pressure restores a number of physical effects absent in §2. The tendency towards condensation is eliminated for all sufficiently large systems. To see this, return to the hydrostatic theory of §2 and the potential well (16). The spherically symmetric (ℓ=0) ground state now obeys

$$\frac{d^2F}{dr^2} + \frac{2}{r}\frac{dF}{dr} = \frac{2M}{\hbar^2}(E-W)F - \frac{2MV_o}{\hbar^2}F^3. \tag{41}$$

If NV_o and ΔW are both large compared with h^2/Mb^2, (41) gives everywhere except near the surface, S, of the well

$$\rho = \rho_\infty = MF_I^2 = MN/v, \tag{42}$$

the corresponding one-particle energy being given by

$$E - W_I = \rho_\infty V_o/M. \tag{43}$$

The fluid is spread out uniformly in the well.

Near S the derivatives of F become large, and the constant solution (42) breaks down. We may follow the argument of §2. Introducing a new healing length

$$a = \hbar(2\rho_\infty V_o)^{-1/2}, \tag{44}$$

writing

$$\xi = n/a, \quad F = X(\xi), \quad W = W_I + (\rho_\infty V_o/M)G(\xi), \tag{45}$$

where $G(\xi)$ is exponentially small for $\xi \to -\infty$, expanding X as

$$X(\xi) = X_o(\xi) + aX_1(\xi) + \ldots, \tag{46}$$

substituting into (15), and equating like powers of a, we obtain

$$d^2X_o/d\xi^2 - [G(\xi) - 1 + (X_o/F_I)^2]\,X_o = 0, \tag{47}$$

$$d^2X_1/d\xi^2 - [G(\xi) - 1 + 3(X_o/F_I)^2]\, X_1 = -\,(C_1^{-1} + C_2^{-1})dX_o/d\xi. \quad (48)$$

Matching at the edges of the boundary layer requires

$$X_o \to 0, \quad X_1 \to 0, \quad \xi \to +\infty; \quad (49)$$

$$X_o \to F_I, \; X_1 \to 0, \quad \xi \to -\infty. \quad (50)$$

Again, explicit solutions generally require numerical integrations, though useful integral relations may be established, for instance

$$\frac{1}{2} F_I^{\,2} = \int_{-\infty}^{\infty} X_o^{\,2} \frac{dG}{d\xi}\, d\xi\ , \quad (51)$$

$$-2\left(\frac{1}{C_1} + \frac{1}{C_2}\right) \int_{-\infty}^{\infty} \left(\frac{dX_o}{d\xi}\right)^2 d\xi = \int_{-\infty}^{\infty} 2X_o X_1 \frac{dG}{d\xi}\, d\xi. \quad (52)$$

Once more, the dominant contribution to the leap in stress across the healing layer arises from the interior solution, although now it is the gas pressure and not the quantum pressure that is mainly responsible. Again, the next largest term can be interpreted as a quantum surface tension, with positive coefficient

$$T_M = 2a\left(\frac{\rho_\infty V_o}{M}\right) \int_{-\infty}^{\infty} \left(\frac{dX_o}{d\xi}\right)^2 d\xi\ . \quad (53)$$

As before, T_M may be estimated[3] from a simple model of X_o. If we suppose that G is a step function of infinite height ($\Delta W = \infty$), (46) may be solved as $X_o = F_I \tanh(-\xi/\sqrt{2})$, and (53) gives

$$T_M \doteq \sqrt{2}\,\hbar^2\rho_\infty/3M^2a. \quad (54)$$

Passing again from 'hydrostatics' to 'hydrodynamics', we note that the gas pressure can supply the restoring force necessary for compressional waves. Perturbing about the static solution (41), we readily find that long wave-length sound propagates at the velocity

$$c = \sqrt{(dp/d\rho)} = \sqrt{(2p/\rho)} = \hbar/Ma\sqrt{2}. \quad (55)$$

At wavelengths of order a and smaller, the quantum pressure increases the phase speed, decreases the group velocity, and introduces weak dispersion.

Vortex lines may be studied as in §2. Unlike their classical counterparts, the cores of these vortices do not have sharply defined surfaces separating regions of zero and non-zero vorticity. All the vorticity they contain is concentrated as δ-functions on their axes. Such a vortex, if classical, would have infinite self-energy. Here, however, the density decreases over the characteristic distance a as the axis is approached, so ensuring a finite tension. The depletion of fluid in the core makes the vortex resemble the classical hollow core model. The permanence of vortex rings implied by the Kelvin-Helmholtz theorem makes them excellent candidates for quasi-particle models, so reviving in a novel context the ideas underlying the vortex atoms proposed by Kelvin in the nineteenth century.

4. STRUCTURE OF THE NEGATIVE ION

It is possible[3,10-12] to account with relative ease for many features of the negative ion by combining the methods of §§2 and 3 above. We use the theory of §1 to represent the electron, regarding w as the potential created by the surrounding condensate; we apply the formalism of §2 to the

<u>exterior</u> of the bubble, taking for W the potential of the electron. More explicitly, we introduce the energy,

$$\int\int U(\vec{x} - \vec{x}')|\psi(\vec{x})|^2|\Psi(\vec{x}')|^2 d\vec{x}d\vec{x}', \tag{56}$$

representing the repulsion of an electron at $\vec{x}$ and a boson at $\vec{x}'$. Taking again the simplest case of a δ-function interaction

$$U(\vec{x} - \vec{x}') = U_o\delta(\vec{x} - \vec{x}'), \tag{57}$$

we then have

$$w(\vec{x}) = \int U(\vec{x} - \vec{x}')|\Psi(\vec{x}')|^2 d\vec{x}' = U_o|\Psi(\vec{x})|^2, \tag{58}$$

$$W(\vec{x}') = \int U(\vec{x} - \vec{x}')|\psi(\vec{x})|^2 d\vec{x} = U_o|\psi(\vec{x}')|^2. \tag{59}$$

By (10) and (58), $\Delta w = U_o\rho_\infty/M$ so that by (22), (23) and (44), $q^2 = mU_o/MV_o$. Equations (1) and (37) become coupled:

$$i\hbar\partial\psi/\partial t = -(\hbar^2/2m)\nabla^2\psi + U_o|\Psi|^2\psi, \tag{60}$$

$$i\hbar\partial\Psi/\partial t = -(\hbar^2/2M)\nabla^2\Psi + (V_o|\Psi|^2 + U_o|\psi|^2)\Psi. \tag{61}$$

As in §2, we define the electronic surface, S, of the bubble by the zero of ψ.

The key to a simple 'hydrostatic' solution of (60) and (61) lies in the fact, which we can verify a posteriori, that the radius, b, of the bubble is large compared with a and a_m, so that the boundary layer methods of §§2 and 3 can be used with minor emendations. We must not forget however that, since the roles of interior and exterior of the bubble have been exchanged for the condensate, the sign of ξ in §3 must be reversed. The mainstream value of F, denoted in §3 by F_I is now written F_S.

To leading order, we set $g(\xi) = X_o^2/F_S^2$ and $G(\xi) = (a^2U_o/F_S^2V_o)x_o^2$ in (26) and (47), as (58) and (59) require. The integral relations (30) and (51) may then be combined to give

$$\frac{a^2}{q^2}\left(\frac{\partial f}{\partial n}\right)_S^2 - \frac{V_o}{2U_o}F_S^2 = \frac{a^2U_o}{F_S^2}[x_o^2X_o^2]_{-\infty}^{\infty} = 0, \tag{62}$$

where we have appealed to (28) and (50). To the next order, the forms of g and G require reconsideration[12]. In place of (27) and (48) we have

$$d^2x_1/d\xi^2 - (q/F_S)^2(X_o^2x_1 + 2x_oX_oX_1) = -(C_1^{-1} + C_2^{-1})dx_o/d\xi, \tag{63}$$

$$d^2X_1/d\xi^2 - (3X_o^2/F_S^2 - 1)X_1 - (a^2U_o/F_S^2V_o)(x_o^2X_1 + 2X_ox_ox_1) = -(C_1^{-1} + C_2^{-1})dX_o/d\xi. \tag{64}$$

The integral consequences (31) and (52) are modified accordingly, and the result (62) is altered to

$$\frac{a^2}{q^2}\left(\frac{\partial f}{\partial n}\right)_S^2 - \frac{V_o}{2U_o}F_S^2 = 2a\left(\frac{1}{C_1} + \frac{1}{C_2}\right)\int_{-\infty}^{\infty}\left[\frac{a^2}{q^2}\left(\frac{dx_o}{d\xi}\right)^2 + \frac{V_o}{U_o}\left(\frac{dX_o}{d\xi}\right)^2\right]d\xi, \tag{65}$$

which now includes the effects of interfacial tension.

The jump conditions (62) or (65) across the boundary layer suffice to match the mainstream electron solution to the mainstream condensate solution. Applied to the electron bubble, we have by (18)

$$f = A(\sin\lambda_I r)/\lambda_I r, \tag{66}$$

showing that $\lambda_I b = \pi$. By (10) the solution is normalized to the first two orders[12] in a/b, if $A^2 = \pi/2b^3$. By (10) and (11) we obtain

$$b = \left(\frac{\pi M^2 a^2}{m\rho_\infty}\right)^{1/5} - \frac{8M^2 a}{5\rho_\infty} \int_{-\infty}^{\infty}\left[\frac{1}{m}\left(a\frac{dx_0}{d\xi}\right)^2 + \frac{1}{M}\left(\frac{dX_0}{d\xi}\right)^2\right] d\xi. \tag{67}$$

It is not at once clear whether b will be decreased by the positive surface tension (53) of the condensate or increased by the negative surface tension (32) of the electron. If we use estimates (33) and (54) however, we see that $|T_m|/T_M$ is of order q^{-1} and, since experiments indicate (§5) that $q < 1$, it appears that the bubble radius should be larger than $(\pi M^2 a^2/m\rho_\infty)^{1/5}$. Direct numerical integrations[12] of x_0 and X_0, and evaluation of the integral seen in (67), suggest that the difference is of the order of a.

The effects of polarization induced by the electron in the surrounding helium can be included by adding[12] to (56) the term

$$-(\tilde{\alpha} e^2/8\pi)\iint |\psi(\vec{x})|^2 |\Psi(\vec{x}')|^2 |\vec{x} - \vec{x}'|^{-4} d\vec{x} d\vec{x}', \tag{68}$$

where $\tilde{\alpha}$ is the polarizability of the helium and e is the electronic charge. This has the effect of contracting the bubble by order $\tilde{\alpha} Me^2a^2/4\pi\hbar^2 b^3$. A detailed theory[12] shows that the reduction is of order a/3 in the practically interesting cases.

Further complications arise when the dynamics of the bubble are considered, although the time-scales of interest are usually large enough compared with the electronic frequencies to justify the neglect of $\partial\psi/\partial t$ in (60); see §2. To evaluate the effective hydrodynamic mass, we consider the bubble in steady motion U, at small Mach numbers $\mathcal{M}=U/c$. The electronic radius, b, of the bubble is increased by about $5\mathcal{M}^2$% because of the pressure forces associated with the flow of condensate over its surface. It is also made slightly oblate, with an ellipticity close to $\mathcal{M}^2/2$. Ignoring this effect, it is found that the dipolar back-flow created by the ion coincides with that of a hard sphere whose radius, b_e, is less than the electronic radius, b, by one to two healing lengths:

$$b_e = b - (aM/\rho_\infty)\int_{-\infty}^{\infty} X_0^{\,2}(\xi)d\xi. \tag{69}$$

It is this radius, rather than b, that determines the induced mass of the ion.

Further details of the calculations outlined above may be found in the paper by Roberts and Grant already cited[12]. We conclude this section by breaking new ground. We consider the oscillations of the bubble, their implications for phonon-ion collisions, and the mobility of negative ions at low temperatures. We again adopt the boundary layer methods described above but, of course, retain the term $\partial\Psi/\partial t$ in (61), so introducing a velocity potential, Φ, in the condensate. We retain only the dominant part of the boundary layer structure, excluding both surface tension and polarization effects. We write,

$$f = f_0 + \alpha a f', \quad F = F_0 + \alpha a F', \quad \Phi = \alpha\Phi', \tag{70}$$

where the suffix o stands for the steady solution obtained earlier, and the terms in α represent time-dependent perturbations, where $0 < \alpha \ll 1$.

It is readily seen from (7) and (40) that Φ' and F' both obey the acoustic wave equation

$$\partial^2\Phi'/\partial t^2 = c^2\nabla^2\Phi'. \tag{71}$$

We could, by following Celli, Cohen and Zuckerman[13], examine solutions in the form of outgoing waves. The eigenfrequencies would be complex, because of the reduction in oscillation amplitude at a point fixed in space as the energy of surface motion is radiated to infinity. The corresponding eigenfunction must tend to infinity with r since, the more distant a wave is, the earlier it must have left the surface, and the greater the amplitude of surface oscillation must then have been. We will not consider solutions of this type below. We will confine our attention to the scattering problem in which an incoming plane wave travelling in the z-direction

$$S'_{INC} = \exp[i(kz-\omega t)], \tag{72}$$

where k and $\omega = ck$ are real, is scattered by the bubble into a set of outgoing waves. We first aim to calculate the scattering amplitude, $h_\ell(k)$, of the ℓth partial wave[13]

$$h_\ell = \frac{1}{1+iQ_\ell}, \quad Q_\ell = \frac{kby_\ell(kb) + K_\ell y_\ell'(kb)}{kbj_\ell(kb) + K_\ell j_\ell'(kb)}, \tag{73}$$

where $y_\ell(z)$ is the spherical Bessel function of the second kind and K_ℓ is the spring constant of the bubble for this mode. We then use h_ℓ to compute the differential cross-section[14] of the bubble

$$\sigma(k,\Theta) = k^{-2}\left|\sum_{\ell=0}^{\infty}(2\ell+1)h_\ell(k)P_n(\cos\Theta)\right|^2, \tag{74}$$

and hence the momentum-transfer cross-section[14]

$$\sigma_T(k) = \iint\sigma(k,\Theta)(1-\cos\Theta)\sin\Theta d\Theta d\chi. \tag{75}$$

From this we finally evaluate the mobility, μ_e, of the ion from[14]

$$\frac{e}{\mu_e} = -\frac{\hbar}{6\pi^2}\int_{-\infty}^{\infty}\sigma_T(k)\frac{\partial n(k)}{\partial k}k^4 dk, \tag{76}$$

where

$$n(k) = [\exp(\hbar ck/KT) - 1]^{-1}, \tag{77}$$

is the density of phonons (in $\hbar\vec{k}$-space) at temperature T. Here K is Boltzmann's constant.

To determine the spring constants, K_ℓ, we have to match solutions of (71) across the boundary layer on S′, the deformed electronic surface, to the quasi-static solutions (18) of the electron mainstream. We first consider the case $\ell \geq 1$. The fact that

$$\psi = A_0 j_0(\lambda_I r) + \alpha a A' j_\ell(\lambda_I r)\, Y_\ell(\Theta,\chi), \tag{78}$$

implies that S′ has the equation

$$r = b(\Theta,\chi,t) \equiv b_o + \alpha a b'(t) Y_\ell(\Theta,\chi), \tag{79}$$

where (using $\lambda_I b_o = \pi$)

$$b'/b_o = j_\ell(\pi)\, A'/A_o. \tag{80}$$

We will continue to refer the boundary layer structure to the unperturbed position, S_o, of the electronic surface, and not to S′. We introduce x′, X′ and η′, the boundary layer forms of f′, F′ and Φ′, and expand these in ascending powers of a

$$x' = a^{-1}x_o' + x_1' + \ldots, \quad X' = a^{-1}X_o' + X_1' + \ldots, \quad \eta' = \eta_o' + a\eta_1' + \ldots, \tag{81}$$

where the coefficients shown depend on t and $\xi = (r - b_o)/a$ and parametrically on Θ and χ. We substitute these into the boundary layer forms of (60) and (61) which, in the Madelung framework, give to the first two orders

$$\partial^2 x'/\partial\xi^2 - (q/F_S)^2(X_o{}^2 x' + 2x_o X_o X') = -(2a/b)\partial x'/\partial\xi, \qquad (82)$$

$$\partial^2 X'/\partial\xi^2 - (3X_o{}^2/F_S{}^2 - 1)X' - (a^2 U_o/F_S{}^2 V_o)(x_o{}^2 X' + 2X_o x_o x') =$$
$$= -(2a/b)\partial X'/\partial\xi + (M/F_S{}^2 V_o)X_o \partial\eta'/\partial t, \qquad (83)$$

$$X_o \partial^2\eta'/\partial\xi^2 + 2(dX_o/d\xi)\partial\eta'/\partial\xi = -(2a/b)X_o\partial\eta'/\partial\xi - 2a^2\partial X'/\partial t. \qquad (84)$$

It seems clear from (84) that $X_o{}^2\partial\eta_o{}'/\partial\xi$ is independent of ξ and, since there is no net condensate flow through the boundary layer at any point, that constant must be zero. Thus η_o' takes throughout the boundary layer the main-stream value Φ_S' of Φ, evaluated on S_o. The right-hand side of (83) does not contribute to leading order in a, and (82) and (83) may be solved to give

$$x_o{}' = \zeta dx_o/d\xi, \quad X_o{}' = \zeta dX_o/d\xi, \qquad (85)$$

where ζ is independent of ξ. These forms represent a net displacement of the equilibrium boundary layer from S_o to S', without change of form; we conclude that $\zeta = -b'Y_\ell$.

In proceeding to the next order we note that, since the velocity of sound (55) is of order 1/a, the time derivatives in (83) and (84) now contribute. In fact, excluding again a net flux of condensate through the boundary layer, (84) shows that $\partial\eta_1{}'/\partial\xi$ takes the value $-a^2\partial\zeta/\partial t$ throughout, and in particular on the outer edge ($\xi = \infty$) of the boundary layer. It follows that

$$a\partial b'/\partial t = (\partial\Phi'/\partial r)_S, \qquad (86)$$

an equation with an obvious interpretation. The equations (82) and (83) again admit an integral, namely

$$\frac{MX_o{}^2}{2U_o F_S{}^2}\ \frac{\partial\eta_o{}'}{\partial t} = \frac{a^2}{q^2}\left[\frac{dx_o}{d\xi}\frac{\partial x_1{}'}{\partial\xi} - x_1{}'\frac{d^2x_o}{d\xi^2}\right]_{-\infty}^{\xi} + \frac{V_o}{U_o}\left[\frac{dX_o}{d\xi}\frac{\partial^2 X_1{}'}{\partial\xi^2} - X_1{}'\frac{d^2X_o}{d\xi^2}\right]_{-\infty}^{\xi}. \qquad (87)$$

On taking the limit $\xi \to +\infty$, and using (18) to evaluate the contributions from the lower limits, we find

$$\partial\Phi_S{}'/\partial t = c^2 K_\ell a b'/b_o, \qquad (88)$$

where

$$K_\ell = \begin{cases} 5/2, \text{ if } \ell = 0; \\ 1 - \ell + \pi j_{\ell-1}(\pi)/j_\ell(\pi), \text{ if } \ell \geq 1. \end{cases} \qquad (89)$$

The numerical values of K_ℓ for the first 20 values of ℓ are given in table I. That of K_o was obtained from an analysis too similar in spirit to the one just described to be repeated here. It may be noted that K_1 is zero, representing the fact that the bubble is neutrally stable to a uniform displacement. Equations (86) and (88) are applied on S_o, and provide the boundary conditions to which solutions of (71) must be subjected.

We developed a program for an Hewlett-Packard 9820 A desk computer to evaluate $\sigma_T(k)$ and μ_e from an arbitrary set of the spring constants. The results were tested with the values ($K_0 = 0.23474$; $K_1 = 0$; $K_2 = 0.45045$; $K_n = 0$, $n>2$) used by Baym, Barrera and Pethick[14], and good agreement was obtained. The programme was then used to generate the results shown in Figures 1 and 2. The effect of truncating series (74) at $\ell = 2$ and $\ell = 19$ are shown in both cases. The prominent peak in $\sigma_T(k)$ seen in Figure 1 is due to a d-wave resonance ($\ell = 2$). A new minor peak is added every time ℓ is incremented by 1. The curve appears to approach its geometrical value[15] ($\sigma_T/4\pi b_o^2 \to 1/2$) with an oscillation of amplitude $(kb_o)^{-2/3}$ and period $2^{-1/3}$. In Figure 2, we see $\mu_e T^3$ plotted in units of L_o, as a function of T measured in units of T_o where

$$T_o = \hbar c/b_o K, \qquad L_o = 3\pi e\hbar^2 c^3/2b_o K. \tag{90}$$

TABLE 1
Spring Constants

ℓ	K_ℓ	ℓ	K_ℓ
0	2.500000000	10	11.56327795
1	0.000000000	11	12.59928101
2	2.289868134	12	13.62973970
3	3.771253431	13	14.65585350
4	5.032253885	14	15.67849696
5	6.198547165	15	16.69832328
6	7.314641577	16	17.71583055
7	8.400646541	17	18.73140537
8	9.467085072	18	19.74535255
9	10.520037400	19	20.75791573

5. EXPERIMENTAL COMPARISONS

The condensate model of helium II is essentially a theory having only one disposable parameter, namely the pseudo-potential, V_o, or equivalently the healing length, a. It is natural to seek to choose this so that theory and observation are in optimum accord. Clearly a choice of a made to fit one physical phemomenon well is likely to conflict with others, and an overall consistency with the experimental facts is not to be anticipated. One notes particularly that, since the condensate is a gas obeying the equation of state (39), we should not expect the theory to perform well at the vapor pressure.

One can obtain an estimate of $V_o = 4\pi d\hbar^2/M$ from measurements of the atomic diameter, d, by α-particle scattering experiments. Values of d of about 2.7 Å have been found. If ρ_∞ is 0.145 g/cm³, the healing length would be 0.82 Å, leading to too small a velocity of sound. One popular procedure has been to extract a from accurate experimental determinations of the relation between the velocity and energy of circular vortex rings. This had led to estimates of a ≑ 1.28 Å, giving much too small a value of c. The reliability of the approach can, however, be questioned. One would have expected a to decrease with increasing pressure, but the reverse seems to be true[16]. It is now believed[17] that the core of a superfluid vortex is the seat of excitations (normal fluid), and that the surface of a vortex core marks the distance from the axis at which the Landau critical velocity is reached, rather than a quantum healing distance; such a belief is consistent with the increase of a with ρ_∞.

Perhaps the most satisfactory way of estimating a is through the velocity of sound (55). To give an example, if we take $c = 238$ m/s, we obtain $a \doteq 0.47$ Å and for $\rho_\infty = 0.145$ g/cm^3 we find that $V_0 \doteq 1.7\ 10^{-37}$ g cm^5/s^2, a value admittedly three times larger than the scattering experiments suggest, and moreover one which will alter as c and ρ_∞ change through applied pressure. Nevertheless, by using c to determine a, we obtain a coefficient of surface tension, T_M, from estimate (54) of 0.37 g/s^2, which is in good agreement with the experimental value of 0.34 g/s^2 at low temperatures.

Turning to the bubble, we see that, in the first approximation, the theory does not require a knowledge of the pseudo-potential, U_0, either for its equilibrium structure or for its oscillation spectrum. The radius, $(\pi M^2 a^2/m\rho_\infty)^{1/5}$, predicted by the first approximation is somewhat small, 11.8 Å using the values quoted above. Since c and ρ_∞ increase with increasing pressure, p, this radius decreases with increasing pressure, although somewhat more slowly than experiments indicate. The bubble radius is increased when the effects of surface tension are added. Unfortunately, Grant and Roberts[12] did not examine values of a as small as 0.47 Å, so that the value of the integral appearing in (67) is not known. Using our earlier estimates, however, it appears that b will be increased to about 13.3 Å by surface tension effects. Table 2 gives $\mu_e T^3$ for a few values of T for both the $\ell = 2$ and the $\ell = 19$ truncations, and for values of b of 11.8 Å, 13.3 Å and 16.0 Å. At the $\ell = 2$ level of truncation, there is a clear tendency for $\mu_e T^3$ to approach a limiting value, of about 36 cm^{2}K^{3}Vs in the case of the 16 Å bubble, as T increases. The explanation of this behavior was provided by Baym, Barrera and Pethick[14] in terms of the shape of the d-wave resonance of Fig. 1. Not surprisingly in view of the very different form of σ_T obtained at $\ell = 19$ truncation, the constancy of $\mu_e T^3$ is not as marked at this level. Nevertheless, the values shown for $\ell = 19$ in Table 1 are not ridiculously far from the experimental value[18] of about 32.5 cm^{2}K^{3}Vs in the range of T in which Baym, Barrera and Pethick measured the success of the work.

When we take the theory of the bubble to the second approximation, a new disposable parameter enters, namely the psuedo-potential, U_0, or equivalently $q = a/a_m$, a relation we can also write as $q^2 = mU_0/MV_0$. Roughly speaking q, as the ratio of the two healing lengths, measures the relative penetration of the condensate wavefunction into the cavity to the penetration of the electron wavefunction into the condensate. If q were zero, it would be legitimate to treat the condensate as an abrupt edge and only consider the electronic boundary layer of §2. At first sight it might appear that, since q^2 is proportional to $m/M \doteq 1.37\ 10^{-4}$ it would be admissible to follow Celli, Cohen and Zuckerman[13] in taking this view. The indications are, however, that U_0/V_0 is large. Scattering experiments give an electron-helium scattering length, λ, of about 0.60 Å, implying that $U_0 = 2\pi\lambda\hbar^2/m$ is about $4.6\ 10^{-35}$ g cm^5/s^2. Taken with the experimental value of $5.7\ 10^{-38}$ g cm^5/s^2 for V_0, we obtain $U_0/V_0 \doteq 810$ and $q \doteq 0.33$. It would be interesting to see whether the effect of restoring q to the Celli-Cohen-Zuckerman theory would have serious repercussions. The indications are that it would not.

The neglect of q in the condensate theory described here would eliminate the condensate surface tension, T_M, and transform the interfacial boundary layer into the structure considered in §2. The associated negative surface tension, T_m, would tend to expand the bubble, an effect confirmed by the calculations of Grant and Roberts[12]. All influences of interfacial tension are, however, of second order in the condensate theory. In the approach of Celli, Cohen and Zuckerman[13], the interfacial tension, σ, is a first order effect.

These authors regarded σ as a disposable parameter that could be legitimately chosen to fit the observed bubble radius at the applied pressure of interest. It is easy to verify that the interfacial tension they require is positive and, particularly at higher pressures, several times larger than the condensate surface tension, T_M, considered earlier. It may be wondered why, with this sign difference, the bubble radii they obtain are, being in perfect agreement with experiment, larger than those obtained from the condensate. The answer is to be found in (39). The condensate is a gas and, to obtain agreement with the observed helium densities, it is necessary to choose a large V_o, leading to pressures (39) of the order of 40 atmospheres. In contrast, the Celli, Cohen and Zuckerman theory treats the helium as a classical compressible fluid, not containing the pressure (39), and to avoid large bubble radii at the vapor pressure, a positive interfacial tension is needed. As we have stated above, we regard (39) as an artificial construct of the theory, not to be identified with the applied pressure, and base our comparison with experiment on density and velocity of sound data.

As Schwarz[15] observes, if the spring constants were regarded as disposable parameters, there would be no difficulty in reproducing any ion mobility data precisely. It appears that even the added flexibility given to the theory by the ad hoc interfacial tension, σ, already permits an excellent account of the mobilities. Schwarz[15] has shown that, for their spring constants, the constancy of $\mu_e T^3$ in the range of T of interest is not lost when the truncation level is increased as it is in ours. In comparing our theory with theirs, one must be perplexed by the substantial difference in the spring constants and in the shape of the mobility curve (labelled 'ℓ = 19' in Fig. 2). He must wonder if, in the disappointing form of that curve on the present theory, and in the sensitivity of the mobility itself to the healing length [as evinced by the c-dependence of (90)], the condensate theory has not met its most severe test to date. He may also speculate on the physical basis of the ad hoc interfacial tension required by the other approach to survive its trial by experiment, and also whether the effects of roton-ion collisions at the higher temperatures have been underestimated.

TABLE 2
Ion Mobilities, μ_e
(T in degrees K, $\mu_e T^3$ in units of cm^2K^3/Vs)

ℓ = 2 Truncation						ℓ = 19 Truncation					
b_o=11.8 Å		b_o=13.3 Å		b_o=16.0 Å		b_o=11.8 Å		b_o=13.3 Å		b_o=16.0 Å	
T	$\mu_e T^3$	T	$\mu_e T^3$	T	$\mu_e T^3$	T	$\mu_e T^3$	T	$\mu_e T^3$	T	$\mu_e T^3$
0.34	229.	0.37	117.	0.31	97.0	0.32	265.	0.33	158.	0.35	70.5
0.41	131.	0.45	77.2	0.43	51.8	0.37	178.	0.42	84.9	0.39	59.0
0.51	86.7	0.52	62.3	0.53	41.7	0.48	95.3	0.46	71.0	0.43	49.0
0.58	70.0	0.56	56.9	0.58	39.5	0.52	79.7	0.52	59.0	0.50	40.0
0.63	63.9	0.64	50.2	0.65	37.6	0.58	66.2	0.57	51.1	0.59	33.1
0.72	56.3	0.70	47.5	0.73	36.6	0.64	57.3	0.71	39.8	0.70	28.1
0.78	53.4	0.78	45.2	0.78	36.5	0.80	44.7	0.85	33.8	0.83	24.6
0.98	49.5	0.94	43.9	0.95	37.4	1.01	36.0	1.01	29.6	1.02	21.0
1.18	49.7	1.15	45.0	1.16	39.9	1.13	30.1	1.13	26.8	1.14	19.4

ACKNOWLEDGEMENT

I am extremely grateful to Professor Russell J. Donnelly for his criticism of this work, and particularly for his contributions to §5. The work described was supported by the Air Force Office of Scientific Research under grant AF-AFOSR-71-1999 and by the National Science Foundation under grant NSF GH 35898.

REFERENCES

1. R. J. Donnelly, "Experimental Superfluidity," Chicago University Press, Chicago (1967).
2. A. L. Fetter, "The Physics of Liquid and Solid Helium," ed. K. H. Bennemann and J. B. Ketterson, Wiley, New York (1975).
3. E. P. Gross, "Quantum Fluids," ed. D. F. Brewer, North Holland, Amsterdam (1966).
4. A. L. Fetter and J. D. Walecka, "Quantum Theory of Many Particle Systems," McGraw Hill, New York (1971).
5. E. Madelung, Z. fur Phys. 40, 322 (1927).
6. J. Grant, Ph.D. Thesis, University of Newcastle (1972).
7. J. Grant, J. Phys. A, 6, L151 (1973).
8. S. Putterman, "Superfluid Hydrodynamics," North Holland, Amsterdam (1974).
9. L. M. Hocking and K. Stewartson, Mathematika 18, 219 (1971).
10. R. C. Clark, Phys. Lett. 16, 42 (1965).
11. R. C. Clark, "Superfluid Helium," ed. J. F. Allen, North Holland, Amsterdam (1966).
12. J. Grant and P. H. Roberts, J. Phys. A., 7, 260 (1974).
13. V. Celli, M. H. Cohen and M. J. Zuckerman, Phys. Rev. 173, 253 (1968).
14. G. Baym, R. E. Barrera and C. J. Pethick, Phys. Rev. Lett. 22, 20 (1969).
15. N. F. Mott and H. S. W. Massey, "The Theory of Atomic Collisions," Third Edition, Clarendon Press, Oxford (1965).
16. M. Steingart and W. I. Glaberson, Phys. Rev. A., 5, 985 (1972).
17. W. I. Glaberson, J. Low Temp. Phys. 4, 289 (1969).
18. K.W. Schwarz and R. W. Stark, Phys. Rev. Lett. 21, 967 (1968).
19. K. W. Schwarz, Phys. Rev. A., 6, 1958 (1972).

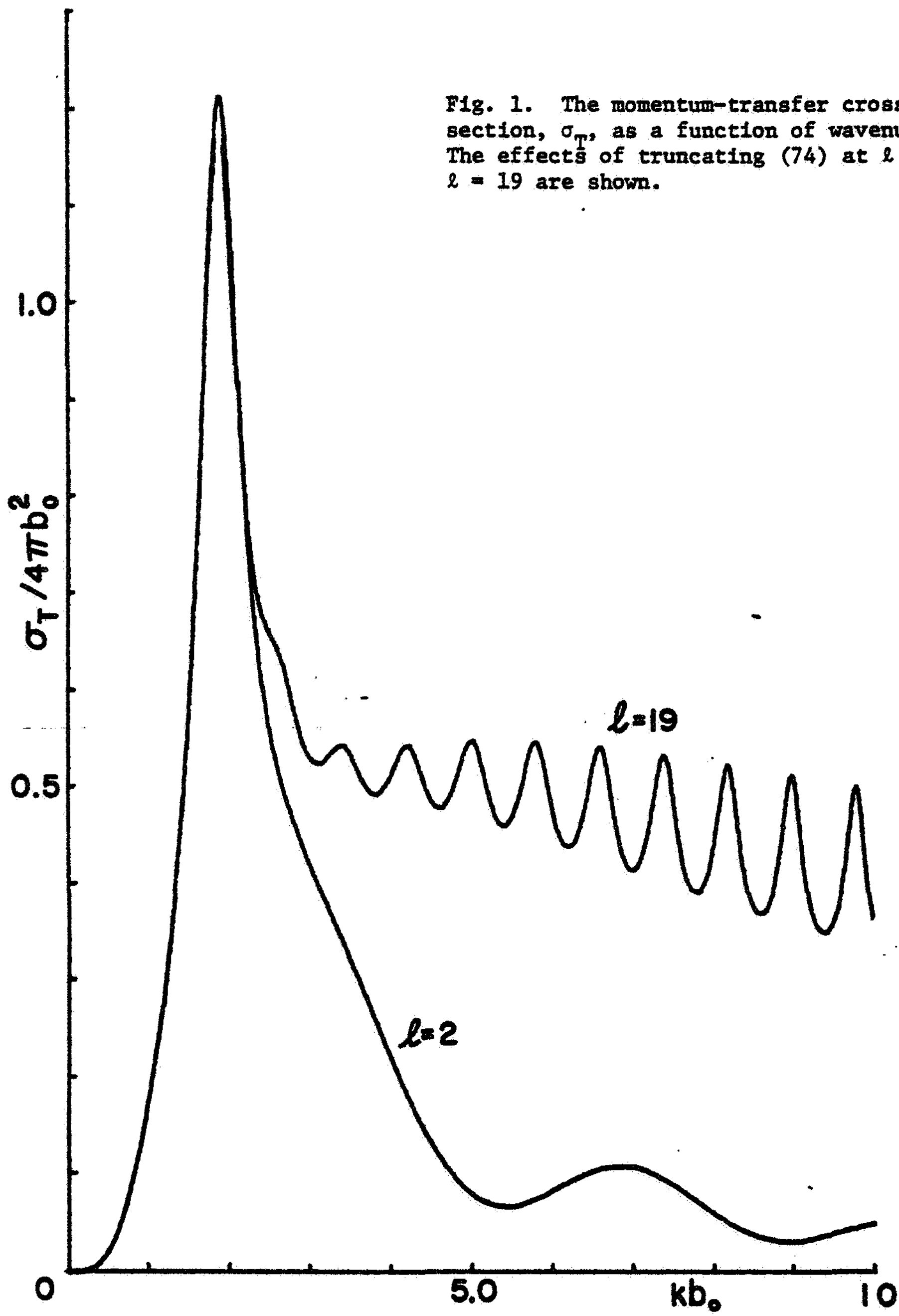

Fig. 1. The momentum-transfer cross-section, σ_T, as a function of wavenumber, k. The effects of truncating (74) at $\ell = 2$ and $\ell = 19$ are shown.

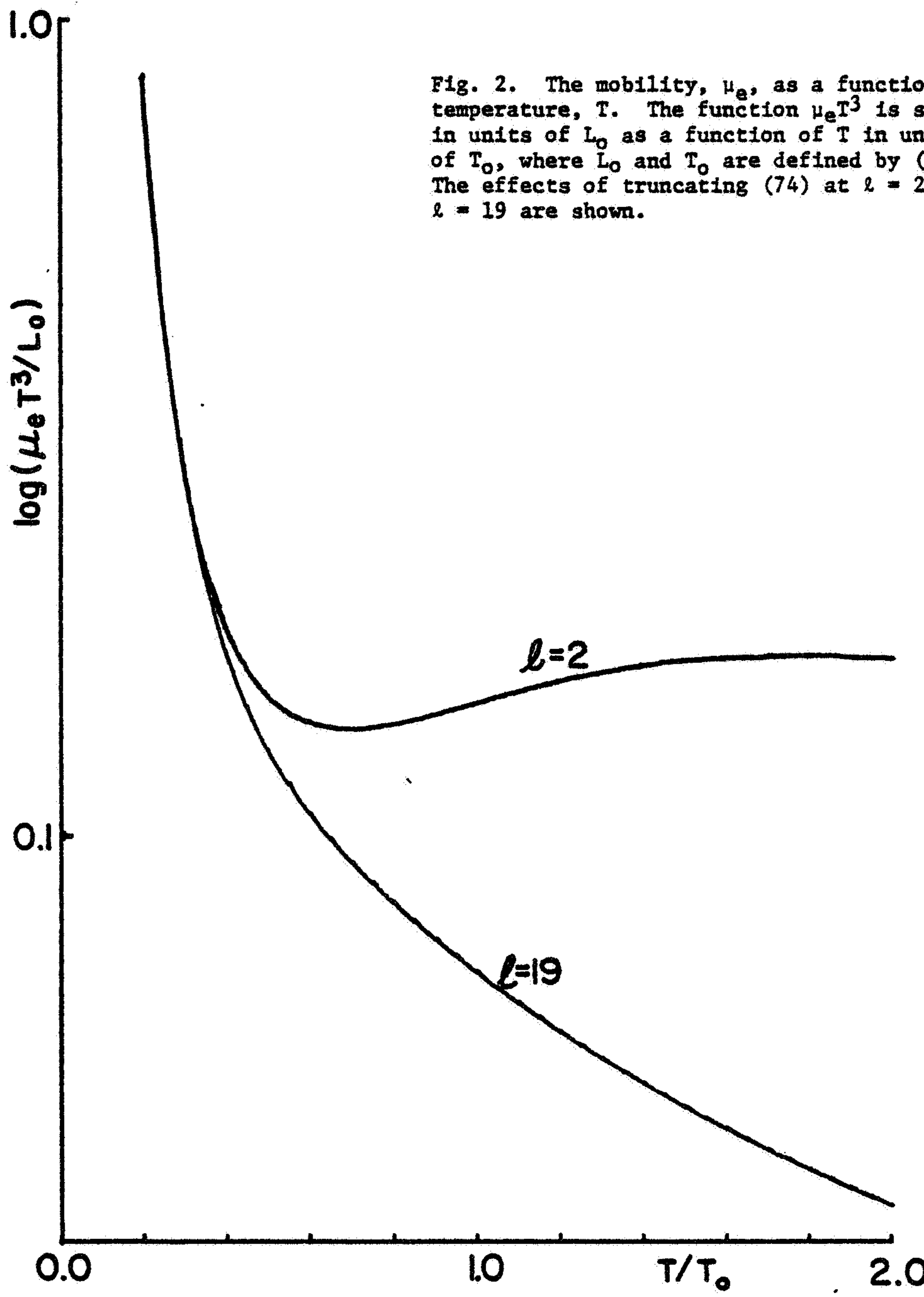

Fig. 2. The mobility, μ_e, as a function of temperature, T. The function $\mu_e T^3$ is shown in units of L_o as a function of T in units of T_o, where L_o and T_o are defined by (90). The effects of truncating (74) at $\ell = 2$ and $\ell = 19$ are shown.